Sustainable Materials Based on Cellulose from Food Sector Agro-Wastes

T. Côto[1], I. Moura[1], A. de Sá[1*], C. Vilarinho[2] and A. V. Machado[1]
[1]*Institute of Polymers and Composites (IPC) and Institute of Nanostructures, Nanomodelling and Nanofabrication (i3N), University of Minho, Campus de Azurém, 4800-058 Guimarães, Portugal*
[2]*Mechanical Engineering Department, University of Minho, Campus de Azurém, 4800-058 Guimarães, Portugal*

ABSTRACT: Biopolymers exhibit unique properties and can be produced from plants' and crops' wastes. Cellulose has been used for the production of sustainable materials, nevertheless due to the difficulty inherent to its extraction, several methods have been studied in order to optimize the process. Therefore, this paper reports the extraction of natural polymers from food sector agro-food wastes, including cellulose, following a green chemistry aproach. The cellulose extracted from pumpkin peel was acetylated and dispersed in a polylactic acid (PLA) matrix. The developed materials were characterized in terms of their structure, morphology and thermal stability. The results demonstrated the efficient chemical modification of cellulose and confirmed its good dispersion within the PLA matrix.

KEYWORDS: Food sector agro-wastes, cellulose, ionic liquid, acetylation, polylactic acid, bioplastics

1 INTRODUCTION

Since the industrial revolution, in particularly after the Second World War, the breakthrough in materials' research increased fast, resulting in the wide use of non-conventional materials (1). Petroleum-based synthetic polymers have brought many benefits to human life and became popular in several applications, due to their high specific strength, lightness, resistance to water and water-borne microorganisms, along with their long durability (2, 3). The annual plastic production reached 322 million tons in 2015 (4), and is associated with regional and global environmental problems ranging from air, water and soil pollution, to climate changes (2, 5). Such drawbacks are progressively becoming more visible, competing with the advantages of these products. The most obvious is the amount of plastic waste generation, which could persist for hundreds or even thousands of years. When disposed of, plastics are subjected to environment degradations, break down into toxic micro fragments, and easily spread in the surrounding ecosystems, which can then be assimilated by animals, threatening human health (6, 7). Moreover, petroleum is currently the main feedstock for plastics production, which represents a "source" limitation. Additionally, they are limited by their "fate"; due to the high costs related to the correct collection, removal, disposal, and recycling. Thus, renewability and biodegradability have become a key criteria for sustainable plastic production and consumption (8). To plastics industry it is now mandatory to seek for alternative sustainable sources of raw materials and cost-effective fabrication processes of environmental degradable plastic (9, 11).

Agriculture crops have been used as alternative sources of polymers, but agricultural potential of Earth is limited. Therefore, it is necessary caution to avoid competition with food crops. In this context, agro-food wastes industry appears as an alternative sustainable and continuous source of polymers. Europe produces enormous amounts of inedible residues, more than 24 million tons per year, which are rich in natural polymers, in particular cellulose (12). Among these agro-wastes, food, halum and stems of vegetables/fruits, grains and seeds (13), can be highlighted. The extraction of high purity cellulose from food-wastes is still a challenge. Conventional processing methods cannot be used, leaving industry to resort for cellulose derivatives, consuming extra time and need for costly chemical purification steps to regenerate it.

Bayer and co-workers (5) showed that trifluoroacetic acid (TFA), a natural organic acid with low toxicity that can be biodegraded by microbial action, is capable of extracting cellulose bioplastic. Green solvents, such as the organic salts known as ionic liquids (ILs), have received attention as promising solvents for lignocellulose pretreatment or fractionation (14).

Several studies have been performed aiming to use food sector agro-wastes to produce biodegradable plastics or to be used as reinforcement. Belgacem (15) studied the use of modified cellulose as reinforcement in composites. They found that the modification of cellulose's surface allowed the formation of covalent bonds between the surface and the macromolecular matrix. Recently, Nourbakhsh (16) studied the effect

**Corresponding author: sa.arsenio@gmail.com*

DOI: 10.32604/JRM.2018.00006

of different concentrations of cellulose fibres in a wood-plastic composite. It was found that the addition of 30% and 40% of reinforcement fibres to the plastic matrix resulted in higher modulus and strength. Mostafa (17) used flax fibre agro-wastes as raw material, aiming to produce a cellulose derivative, cellulose acetate (CA).

The present work aims to extract cellulose from pre-treated pumpkin peel, a byproduct of agro-food wastes, using the IL 1-butyl-3-methylimidazolium chloride [(BMIM)Cl], which can be infinitely recycled and is amenable to solvation at room temperature, making it an excellent green solvent. Additionally, cellulose was chemically modified to cellulose acetate, which was then dispersed in polylactic acid (PLA). The extracted cellulose and the resulting PLA composite were characterized using several analytical techniques, such as ^{1}H NMR, FTIR, Raman, SEM and TGA. The results showed that the chemical modification of the cellulose through an acetylation process was successfully achieved and allowed a good dispersion in the PLA matrix.

2 MATERIALS AND METHODS

2.1 Materials

Pumpkin peel was collected from vegetable crops. Sodium hydroxide (NaOH) pellets and methanol (MeOH, 99.5%) were acquired from Panreac. Hydrogen peroxide (H_2O_2, >30% w/v), iodine (I_2, 99.9+%) and ethanol (EtOH, 99.99%) were purchased from Fisher Chemicals. Acetic anhydride [$(CH_3CO)_2O$, 98+%], sodium thiosulfate (99%), deuterated dimethylsulfoxide (DMSO-d_6) and cellulose acetate (Mw=100 000 g/mol) were purchased from Acros Organics. 1-butyl-3-methylimidazolium chloride {[(BMIM)Cl], ≥95%}, and the dichloromethane (DCM, ≥99.9%) were acquired from Sigma-Aldrich. PLA (M_w=195 000 g/mol) was acquired from Novamont®, Italy. Deionized water was obtained from a Milli-Q Advantage A10 Ultrapure Water Purification device.

2.2 Chemical Pretreatment

A chemical pretreatment was performed to solubilize the hemicellulose and pigments. Briefly, 1 g of dry pumpkin peel residue was suspended in 50 mL of 2 wt.% NaOH solution and stirred during 4 h at 100ºC. Hydrogen peroxide was used to remove pigments, using 80 mL of 0.5 M NaOH containing 2% (v/v) of H_2O_2 per each gram of material. The solution was stirred during 1 h. Then, 20 mL of 2 M NaOH solution was added and the suspension stirred during 5 h at 55ºC. Then, the residue was washed with distilled water until achieve neutral pH, allowing to remove the impurities. Finally, the residue was filtered and dried in a vacuum oven, at 60ºC, overnight (18-21).

2.3 Cellulose Dissolution Using Ionic Liquid

The ionic liquid 1-butyl-3-methylimidazolium chloride [(BMIM)Cl], previously molten at 70ºC, was used as a green solvent to isolate cellulose.

12 mL of [(BMIM)Cl] was used per each 0.25 g of material. The mixture was placed in a thermostatic bath, under vigorous stirring, at 90ºC until complete dissolution (approximately 24 h). Then, distilled water was added to promote cellulose's precipitation, at 80ºC under vigorous stirring. The resulting mixture was separated by decantation and the solid fraction centrifuged during 10 min, using a rotor speed of 12 000 rpm. The resulting material was washed several times with distilled water to remove residual IL. Finally, it was dried in a vacuum oven, at 60ºC, overnight.

2.4 Cellulose Acetylation

The acetylation of cellulose was preformed according to Archana et al. (21). Briefly, 0.2 g of precipitated cellulose was suspended in 10 mL of acetic anhydride and an excess of iodine (0.3 g) were added to the mixture. The reaction was carried out, at 80ºC, during 5 h, under stirring. Then, the mixture was cooled in an ice bath, and 5 mL of saturated sodium thiosulfate aqueous solution was added to neutralize the catalyst, following the colour change from dark brown to colourless. After this, 30 mL of EtOH were added and the mixture stirred during 1 h, aiming to remove residual compounds and by-products. Several washings with 75% (v/v) EtOH and distilled water were performed to assure the complete removal of undesired contaminants. Then, the solid fraction was collected and dried in a vacuum oven, at 60ºC, overnight. Thereafter, this fraction was dissolved in DCM, allowing to isolate CA from the remaining compounds, by filtration. The DCM fraction was placed in a petri dish and dried in the vacuum oven until complete solvent evaporation, affording a film of CA. The remaining acetic anhydride was removed with MeOH and the CA dried in a vacuum oven, at 60ºC.

2.5 Development of Renewable Acetylated Cellulose-based Materials

0.02 g of CA was added to a solution of PLA (0.18 g) in DCM (25 mL). The mixture was stirred during 1 h, at 50ºC, to promote cellulose acetate dissolution. Then, the mixture was left to rest overnight in the fridge, in

order to eliminate bubbles, before being cast into a flat polytetrafluoroethylene (PTFE) mould. The resulting film was placed in an oven at 40ºC, in order to guarantee the complete solvent evaporation (22).

2.6 Characterization

2.6.1 Fourier transform infrared spectroscopy (FTIR)
Room temperature FTIR spectra were acquired using a 4100 Jasco spectrometer in the range 4500-400 cm^{-1}, by averaging 16 scans and using a resolution of 4 cm^{-1}. An amount of 20 mg of each material was mixed with 200 mg of KBr to prepare translucent sample disks.

2.6.2 Scanning electron microscopy (SEM)
SEM analysis was performed, in order to evaluate the samples' morphology, using a FEI Quanta 400 Scanning Electron Microscope. The samples were previously coated with a gold thin film. The analysis was carried out with a high voltage around 10 kV and under magnification between 1000x and 15000x.

2.6.3 Proton nuclear magnetic resonance (1H NMR) spectroscopy
^{1}H NMR spectroscopy of acetylated cellulose was performed in a 400 MHz Avance Bruker NMR spectrometer equipped with an ultrashield magnet and using deuterated DMSO. The ^{1}H chemical shifts are reported in ppm (parts per million). The residual solvent peak has been used as internal reference.

2.6.4 Raman spectroscopy
Room temperature Raman spectra were acquired in a LabRAM HR Evolution spectrometer equipped with a 532 nm laser (Laser Quantum Torus 532, power 50 to 750 mW). The Raman spectra of the samples were acquired in the range 400-4000 cm^{-1} (acquisition time: 30 s; accumulations: 30; RTD time (s): 10; grating: 600 gr/mm; ND filter: 10%; hole: 200).

2.6.5 Dynamic mechanical analysis (DMA)
DMA tension measurements of PLA and PLA with 10% CA films were carried out with a dynamic mechanical analyser TT-DMA TRITON at a frequency of 1 Hz. The films (20×3 mm) were tested (three different specimens for each sample) with a normal force of 1 N, in the temperature range from 40°C to 100°C, at 5 $^{o}C.min^{-1}$.

3 RESULTS AND DISCUSSION

After drying and grinding, the chemical composition of raw pumpkin peel was evaluated by FTIR spectroscopy (Figure 1A). It was expected that cellulose, hemicellulose and lignin would influence the FTIR spectrum and several typical vibrational bands are consistent with their presence (23, 24). The FTIR spectrum exhibits a broad band centred at 3354 cm^{-1} that was assigned to OH stretching of the intramolecular hydrogen bonds and a peak at 2926 cm^{-1} related to CH stretching. At 1743 cm^{-1} and 1628 cm^{-1} the spectrum shows intense bands typical of C=O and C=C bonds' stretching, respectively, which confirmed the presence of lignin. The 1628 cm^{-1} vibration may also result from the OH bending of water absorbed by the cellulose (25). Vibrational bands at 1370 cm^{-1} are related to the bending of OH groups. Additionally, the band at 1046 cm^{-1} can be associated to the C-O-C stretching in the pyranose rings. The FTIR spectrum of the pretreated residue shows significant differences in the chemical composition relative to raw pumpkin peel (Figure 1B). The major differences are related to the absence of C=O vibrational band at 1743 cm^{-1} and the appearance of two new bands at 1166 cm^{-1} and 898 cm^{-1} that are related with the antisymmetric bridge stretching and the CH deformation characteristic of β-glycosidic linkage for the pretreated sample. This observation is related to the removal of hemicellulose and lignin (20, 23). Furthermore, it can be seen that the OH stretching band, centred at 3398 cm^{-1}, is broader and more intense in the pretreated sample, owing to the hemicellulose removal, since the presence of this compound limits the vibration of cellulose and lignin (23).

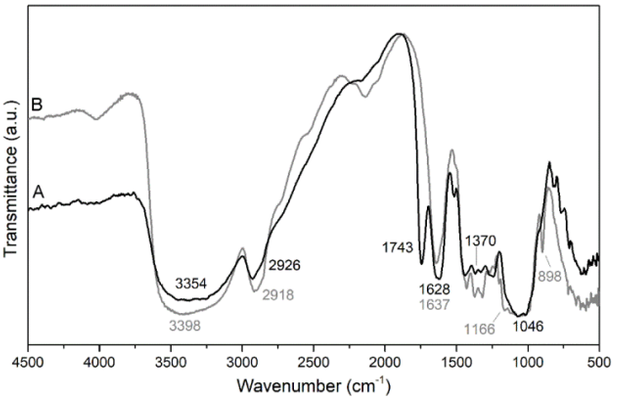

Figure 1 FTIR spectra of raw pumpkin peel before (A) and after chemical pretreatment (B).

Figure 2 demonstrates the effect of the bleaching treatment where it can be noticed that this process allowed to remove pigments and stains. The same effect was observed by Teixeira et al. (26), who performed the same treatment in sugarcane bagasse.

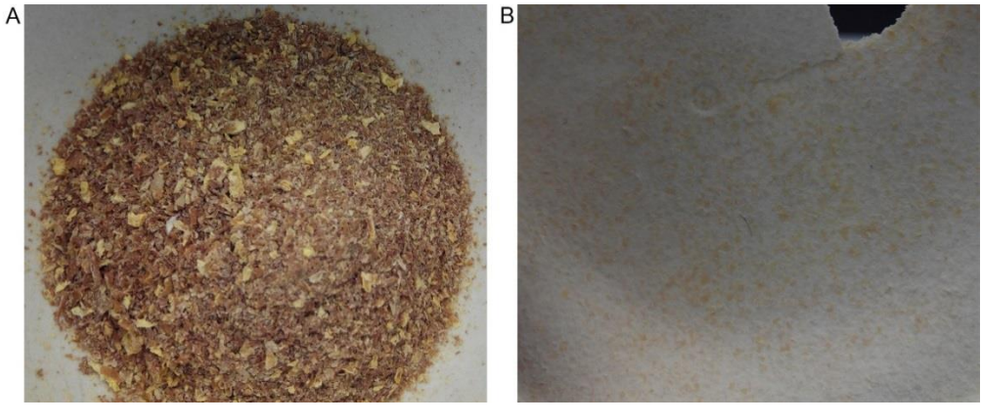

Figure 2 Grinded dry pumpkin peel before (A) and after (B) bleaching. The bleached material formed a brittle plate-like shape during the drying process.

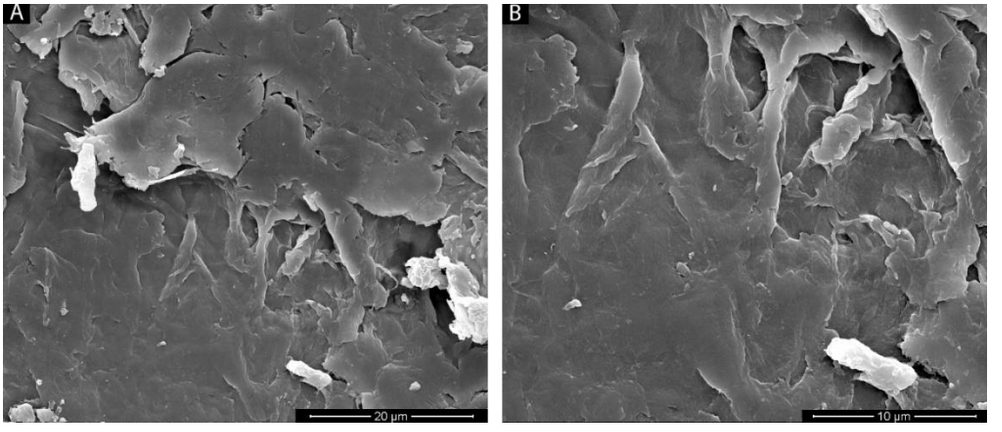

Figure 3 SEM micrographs of chemically pre-treated raw pumpkin peel under 5 000x (A) and 10 000x (B) magnifications.

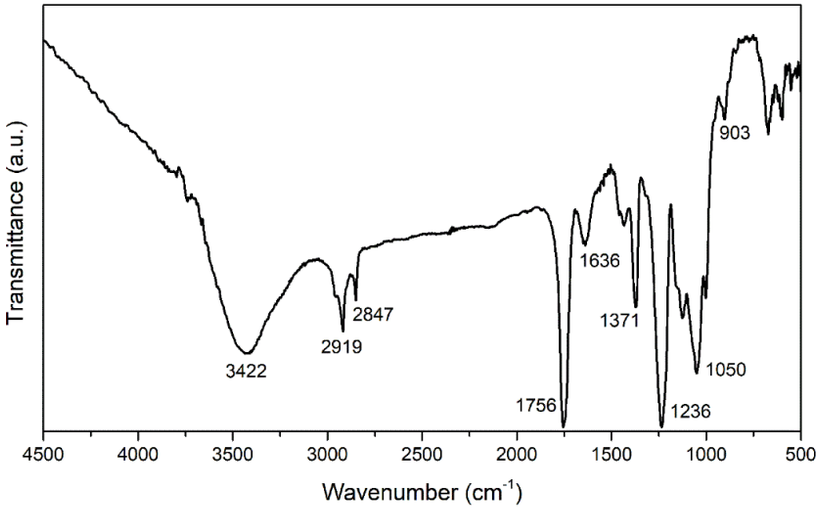

Figure 4 FTIR spectra of acetylated cellulose.

Table 1 Amount of solid fraction recovered after dissolution in IL.

Sample	Solid fraction (%)	Deviation (%)
Raw pumpkin peel	25.5	±3.99
Pretreated raw pumpkin peel	67.8	±9.38

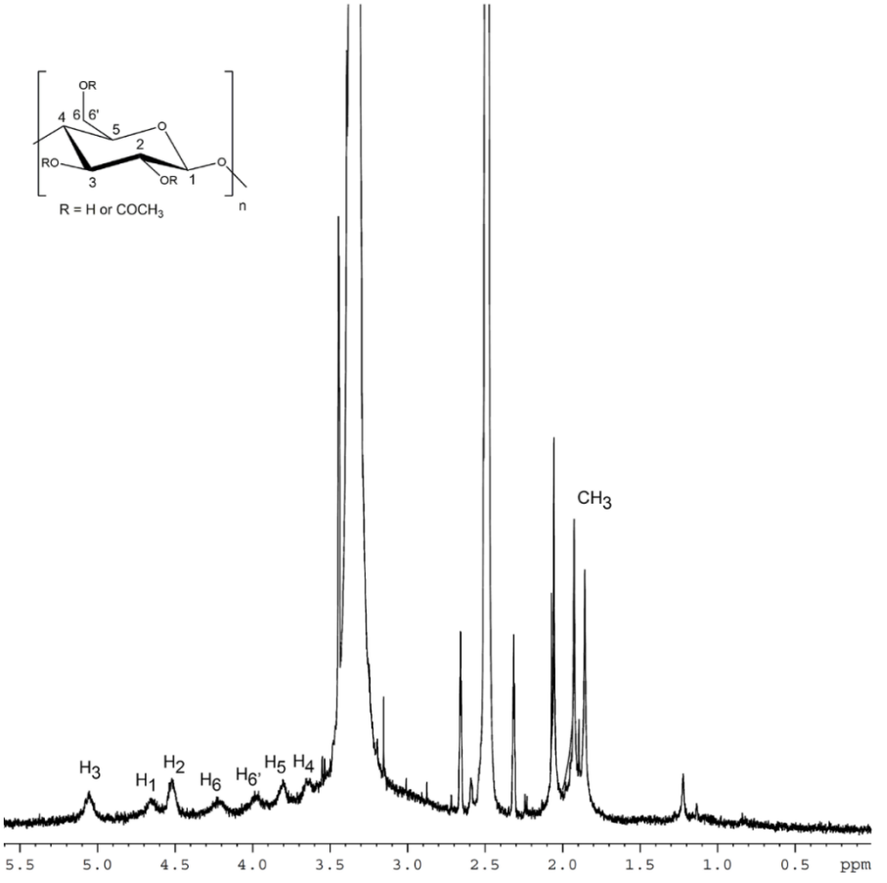

Figure 5 ^{1}H NMR spectrum of acetylated cellulose.

The sample's morphology after the chemical pre-treatment is depicted in Figure 3. It can be noticed a smooth morphology under both magnifications. Modenbach et al. (32) described that chemical pre-treatment using sodium hydroxide promotes hemicellulose hydrolysis and increases the surface area. This is due to the biomass swelling and reduction of the degree of polymerization (DP) and crystallinity. Kumar et al. (28, 33) evaluated the morphological differences between raw sugarcane bagasse before and after potassium hydroxide pre-treatment. They observed cleaner surfaces after pre-treatment that are consistent with hemicellulose removal. Teixeira (34) and Pan (35) performed alkaline pre-treatment with sodium chloride in sugarcane bagasse and wheat straw, respectively, and observed a partial disruption of the residues' structure.

The IL 1-butyl-3-methylimidazolium chloride was used to investigate the amount of cellulose that can be extracted with and without chemical pre-treatment. The amount of solid fraction (SF) extracted was calculated using the following equation and the values are summarized in Table 1.

$$\text{SF}\ (\%) = \frac{\text{mass of final compound (g)}}{\text{mass of initial compound (g)}} \times 100$$

These results demonstrate that the chemical pretreatment allowed to recover almost three times more SF comparatively to the raw pumpkin peel, corroborating the importance of the chemical pretreatment to obtain a higher amount of solid fraction.

This is associated with the hemicellulose removal during the sample pre-treatment that facilitates the contact between the solvent and cellulose, improving its dissolution. Moreover, Mäki-Arvela et al. (31) and Lee et al. (32) reported that [(BMIM)Cl] is a relatively poor solvent for lignin dissolution but suitable for cellulose.

The cellulose acetylation was performed based on the procedure described by Archana et al. (21). A FTIR analysis was performed to confirm the efficiency of the process. Introducing acetyl groups in the chemical structure will result in the observation of vibrational bands typical of this function, namely the C=O and C-O stretching. As it can be seen in Figure 4, the spectrum exhibits a well-defined peak at 1756 cm^{-1} consistent with the presence of C=O moieties. Also, it can be noticed the vibrational band at 1236 cm^{-1}, which is related to C-O stretching. The results confirmed the successful cellulose acetylation and are in agreement with results already reported (21, 33, 34).

The ^1H NMR spectrum of the acetylated cellulose (Figure 5) displays typical NMR resonances consistent with the CA's chemical structure. In the chemical shift range between 3.5 and 5.3 ppm appear resonances, with the indexes H_1 to $H_{6'}$, related to the protons bonded to the carbon atoms of the glycosides groups (35,36). The NMR spectrum also displays typical resonances characteristic of CH_3 groups at 2.2-1.5 ppm. Since cellulose does not contain CH_3 groups, their presence confirms that cellulose acetate was successfully synthesized (35, 36).

The degree of substitution (DS), i.e. the average number of hydroxyl groups that were replaced by acetate groups, was determined based on the methodology reported by Kono (35).

The DS can reach a maximum value of 3, since there are only three hydroxyl groups per each hexose unit in cellulose's repeating unit. Also, the substitution can only occur in the OH groups in position 2, 3 and 6, as it is shown in detail in Figure 5.

A DS of 3 represents 9 protons influencing the CH_3 typical resonance. According to the NMR spectrum, this resonance is associated to a total of 7.25 protons (80.5%), which corresponds to a DS of 2.42.

To confirm the cellulose DS, the corresponding chemical shifts were compared to those observed by Kono (35), who studied the chemical shifts characteristic of cellulose acetate samples with different DS (1 to 3). Additional to the peak's integration, acetylated cellulose also showed NMR resonances with chemical shifts that are in agreement with those reported for a DS between 2 and 3. The results obtained in the present work are also in agreement with the previous study of Das et al. (21), which synthesized cellulose acetate from rice husk with a DS between 2.12 and 2.91.

Figure 6 presents a solvent casting film of the modified cellulose. As it can be seen, the film is transparent and not brittle.

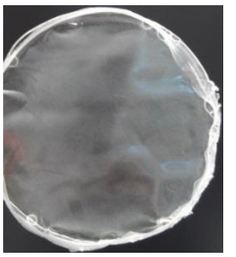

Figure 6 Solvent casting film of acetylated cellulose.

Raman spectroscopy (Figure 7) evidences characteristic peaks of both PLA and acetylated cellulose in the composite. The chemical groups presented in CA and PLA are quite similar, as discussed by Sánchez-Marquéz et al. (37), which difficult the analysis of the Raman spectrum of the final material. Nevertheless, the presence of PLA is confirmed by the OH group at 2881 cm^{-1}, C-CH_3 at 2947 cm^{-1} and CH stretching at 3003 cm^{-1} (38), while the presence of acetylated cellulose is confirmed by the existence of CO_2CH_3 groups related vibrations at 514-658 cm^{-1} and 1740 cm^{-1} (39) and OH groups related vibration at 3560 cm^{-1} (40). These peaks are present, and highlighted, in the acetylated cellulose sample (Figure 7), corroborating that the cellulose acetylation was successfully achieved.

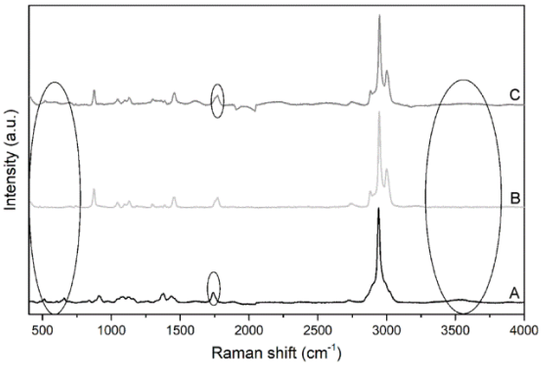

Figure 7 Raman spectra of acetylated cellulose (A), PLA (B), and produced PLA/CA material (C).

SEM micrographs of the composite (Figure 8) confirms the dispersion of acetylated cellulose in the PLA matrix. Moreover, it can be seen that the acetylated cellulose is well impregnated in PLA matrix, indicating a good chemical compatibility and a strong interfacial adhesion between both biopolymers (22).

Yan et al. (50) studied the influence of incorporating nanocrystalline cellulose and acetylated nanocrystalline cellulose into PLA matrix on its morphology. They concluded that acetylation promoted good interface compatibility between the acetylated nanocrystalline cellulose and the PLA matrix, whereas nanocrystalline cellulose without acetylation resulted in a composite with holes, due to the weak compatibility.

Two different phases can be identified in Figure 8, a homogeneous phase attributed to PLA matrix and dispersed cellulose particles. This morphology can be explained based on the dissolution procedure of the acetylated cellulose fibres and on its microcrystalline structure. Lin et al. (22) used acetylated nanocrystalline cellulose to produce nanocomposites and observed that the resulting nanocomposites' morphology was composed by PLA and some agglomerates of acetylated cellulose nanocrystals, which were formed for concentrations higher than 8%. Moreover, it can be seen that the sample exhibits a porous structure, which can be related with the solvent evaporation rate. Terrazas-Bandala et al. (51) and Júnior et al. (12) carried out morphological studies of CA membranes produced by solvent evaporation. They also observed the formation of a porous structure. Altena et al. (8) studied the diffusion rate of CA in different solvents and they proposed that high polymer concentration leads to a decrease in the solvent diffusion rate. Thus, one possible explanation for the existence of a porous structure could be related with the solvent saturation, resulting in a low diffusion rate and, consequently, in a decrease of the evaporation rate.

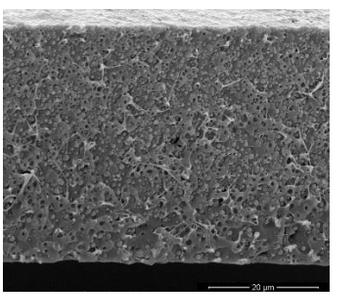

Figure 8 SEM micrograph of the transversal section of the produced (PLA/CA) material under a magnification of 15 000x.

DMA assays were performed for pristine PLA and the blend containing 10% CA in order to evaluate the CA capacity to be used as PLA reinforcement. Figure 8 depicts the films' storage modulus behaviour as a function of the temperature. As can be seen, the addition of 10% of CA enhances the PLA's mechanical properties with an increase of the storage modulus at 40ºC around 40%. This observation proves that the acetylated cellulose can be used as PLA's reinforcement. The addition of acetylated cellulose decreases the polymer chains mobility, since the onset temperature where a drop in the *E'* occurs, or the glass transition temperature, increased from 60ºC to 65ºC. Nevertheless, the loss of stiffness is more abrupt and pronounced for the blend. Similar results were obtained by Jonoobi et al. (52), they also observed an enhancement of the *E'* and an increase of the T_g of PLA reinforced with cellulose nanofibers.

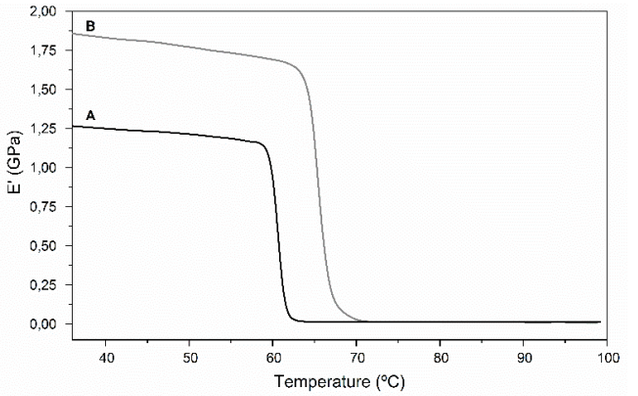

Figure 9 Storage modulus (E') curves obtained by DMA for PLA (A) and PLA with 10% CA films (B).

4 CONCLUSION

Agro-wastes, due to their abundance and composition, are an excellent source of raw material for the preparation of new polymeric systems. This work was focused on the valorisation of food sector agro-wastes, in which a new procedure to isolate cellulose was investigated, consisting in a chemical pre-treatment and the use of a green solvent, an ionic liquid. This combination allowed to obtain almost pure cellulose sample that was afterwards modified in order to enhance the compatibility between cellulose and PLA. The new developed material showed good compatibility between the phases. The PLA's mechanical properties were enhanced with the addition of the acetylated cellulose.

ACKNOWLEDGMENT

This work is funded by FEDER funds through the COMPETE 2020 Programme and National Funds

through FCT-Portuguese Foundation for Science and Technology under the project UID/CTM/50025/2013.

REFERENCES

1. M. Okamoto and B. John, Synthetic biopolymer nanocomposites for tissue engineering scaffolds. *Prog Polym Sci.* **38**(10-11), 1487-503 (2013).
2. T.A. Hottle, M.M. Bilec and A.E. Landis, Sustainability assessments of bio-based polymers. *Polym Degrad Stab.* **98**(9), 1898-907 (2013).
3. K. Majeed, M. Jawaid, A. Hassan, A. Abu Bakar, H.P.S. Abdul Khalil, A.A. Salema et al., Potential materials for food packaging from nanoclay/natural fibres filled hybrid composites. *Mater Des* **46** 391-410 (2013).
4. Plastics Europe. Plastic-the Facts 2016. An Analysis of European Plastics Production, Demand and Waste Data (2016).
5. I.S. Bayer, S. Guzman-Puyol, J.A. Heredia-Guerrero, L. Ceseracciu, F. Pignatelli, R. Ruffilli et al., Direct transformation of edible vegetable waste into bioplastics. *Macromolecules* **47**(15), 5135-5143 (2014).
6. E.L. Teuten, J.M. Saquing, D.R.U. Knappe, M.A. Barlaz, S. Jonsson, A. Björn et al., Transport and release of chemicals from plastics to the environment and to wildlife. *Philos Trans R Soc Lond B Biol Sci.* **364**(1526), 2027-2045 (2009).
7. D.K.A. Barnes, F. Galgani, R.C. Thompson and M. Barlaz, Accumulation and fragmentation of plastic debris in global environments. *Philos Trans R Soc Lond B Biol Sci.* **364**(1526), 1985-1998 (2009).
8. F.W. Altena, J. Smid and C.A. Smolders, Diffusion of solvent from a cast CA solution during skinned membranes formation. *Polymer (Guildf)* **26**(10), 1531-1538 (1984).
9. K. Leja and G. Lewandowicz, Polymer biodegradation and biodegradable polymers-A review. *Polish J Environ Stud.* **19**(2), 255-266 (2010).
10. B. Imre and B. Pukánszky, Compatibilization in bio-based and biodegradable polymer blends. *Eur Polym J.* **49**(6), 1215-1233 (2013).
11. H. Garcia, R. Ferreira, C. Martins, A. F. Sousa, C.S.R. Freire, A. J. D. Silvestre et al., Ex situ reconstitution of the plant biopolyester suberin as a film. *Biomacromolecules* **15**(5), 1806–1813.
12. M.F. Ferreira Júnior, E.A.R. Mundim, G.R. Filho, C. Da Silva Meireles, D.A. Cerqueira, R.M.N. De Assunção et al., SEM study of the morphology of asymmetric cellulose acetate membranes produced from recycled agro-industrial residues: Sugarcane bagasse and mango seeds. *Polym Bull.* **66**(3), 377-389 (2011).
13. A.A. Shah, F. Hasan, A. Hameed and S. Ahmed, Biological degradation of plastics: A comprehensive review. *Biotechnol Adv.* **26**(3), 246-265 (2008).
14. M. FitzPatrick, P. Champagne, M.F. Cunningham and R.A. Whitney, A biorefinery processing perspective: Treatment of lignocellulosic materials for the production of value-added products. *Bioresour Technol* **101**(23), 8915-8922 (2010).
15. M.N. Belgacem and A. Gandini, The surface modification of cellulose fibres for use as reinforcing elements in composite materials. *Compos Interfaces* **12**(1-2), 41-75 (2005).
16. A. Nourbkhsh and A. Ashori, Fundamental Studies on Wood-Plastic Composites: Effects of Fiber Concentration and Mixing Temperature on the Mechanical Properties of Poplar/PP Composite. *Polym Polym Compos* **16**(2), 101-113 (2008).
17. N.A. Mostafa, A.A. Farag, H.M. Abo-dief and A.M. Tayeb, Production of biodegradable plastic from agricultural wastes. *Arab J Chem* (2015) (In Press).
18. M.A. Henrique, H.A. Silvério, W.P. Flauzino Neto and D. Pasquini, Valorization of an agro-industrial waste, mango seed, by the extraction and characterization of its cellulose nanocrystals. *J Environ Manage* **121**, 202-209 (2013).
19. W.P. Flauzino Neto, H.A. Silvério, N.O. Dantas and D. Pasquini, Extraction and characterization of cellulose nanocrystals from agro-industrial residue-Soy hulls. *Ind Crops Prod* **42**(1), 480-488 (2013).
20. H.A. Silvério, W.P. Flauzino Neto, N.O. Dantas and D. Pasquini, Extraction and characterization of cellulose nanocrystals from corncob for application as reinforcing agent in nanocomposites. *Ind Crops Prod* **44**, 427-436 (2013).
21. A.M. Das, A.A. Ali and M.P. Hazarika, Synthesis and characterization of cellulose acetate from rice husk: Eco-friendly condition. *Carbohydr Polym* **112**, 342-349 (2014).
22. N. Lin, J. Huang, P.R. Chang, J. Feng and J. Yu, Surface acetylation of cellulose nanocrystal and its reinforcing function in poly (lactic acid). *Carbohydr Polym* **83**(4), 1834-1842 (2011).
23. B.R. Garcia-Reyes and J.R. Rangel-Mendez, Contribution of agro-waste material main components (hemicelluloses, cellulose, and lignin) to the removal of chromium (III) from aqueous solution. *J Chem Technol Biotechnol* **84**(10), 1533-1538 (2009).
24. N. Sun, M. Rahman, Y. Qin, M. L. Maxim, H. Rodríguez and R. D. Rogers, Complete dissolution and partial delignification of wood in the ionic liquid 1-ethyl-3-methylimidazolium acetate. *Green Chem* **11**(5), 646 (2009).
25. C.F. Liu, R.C. Sun, A.P. Zhang, J.L. Ren and Z.C. Geng, Structural and thermal characterization of sugarcane bagasse cellulose succinates prepared in ionic liquid. *Polymer Degradation and Stability* **91**, 3040-3047 (2006).
26. E.M. de Teixeira, T.J. Bondancia, K.B.R. Teodoro, A.C. Corrêa, J.M. Marconcini and L.H.C. Mattoso, Sugarcane bagasse whiskers: Extraction and characterizations. *Ind Crops Prod* **33**(1), 63-66 (2011).
27. A. Modenbach, Sodium hydroxide pretreatment of corn stover and subsequent enzymatic hydrolysis: An investigation of yields, kinetic modeling and glucose recovery. University of Kentucky (2013).
28. A. Kumar, Y.S. Negi, V. Choudhary and N.K. Bhardwaj, Characterization of Cellulose Nanocrystals Produced by Acid-Hydrolysis from Sugarcane Bagasse as Agro-Waste. *J Mater Phys Chem* **2**(1), 1-8 (2014).

29. A. Kumar, Y.S. Negi, N.K. Bhardwaj and V. Choudhary, Synthesis and characterization of methylcellulose/PVA based porous composite. *Carbohydr Polym* **88**(4), 1364-1372 (2012).
30. C. Guo, L. Zhou and J. Lv, Effects of expandable graphite and modified ammonium polyphosphate on the flame-retardant and mechanical properties of wood flour-polypropylene composites. *Polym Polym Compos* **21**(7), 449-456 (2013).
31. P. Mäki-Arvela, I. Anugwom, P. Virtanen, R. Sjöholm and J.P. Mikkola, Dissolution of lignocellulosic materials and its constituents using ionic liquids-A review. *Ind Crops Prod* **32**(3), 175-201 (2010).
32. S.H. Lee, T.V. Doherty, R.J. Linhardt and J.S. Dordick, Ionic liquid-mediated selective extraction of lignin from wood leading to enhanced enzymatic cellulose hydrolysis. *Biotechnol Bioeng* **102**(5), 1368-1376 (2009).
33. N. Olaru, L. Olaru, C. Vasile and P. Ander, Surface modified cellulose obtained by acetylation without solvents of bleached and unbleached kraft pulps. *Polimery* **56**(11), 11-12 (2011).
34. H. Kamal, F.M. Abd-Elrahim and S. Lotfy, Characterization and some properties of cellulose acetate-co-polyethylene oxide blends prepared by the use of gamma irradiation. *J Radiat Res Appl Sci* **7**(2), 146-153 (2014).
35. H. Kono, H. Hashimoto and Y. Shimizu, NMR characterization of cellulose acetate: Chemical shift assignments, substituent effects, and chemical shift additivity. *Carbohydr Polym* **118**, 91-100 (2015).
36. D.A. Cerqueira, G.R. Filho, R.A. de Carvalho and A.J. M. Valente, Caracterização de acetato de celulose obtido a partir do bagaço de cana-de-açúcar por 1H-RMN. *Polímeros* **20**(2), 85-91 (2010).
37. J.A. Sánchez-Márquez, R. Fuentes-Ramírez, I. Cano-Rodríguez, Z. Gamiño-Arroyo, E. Rubio-Rosas, J.M. Kenny et al., Membrane made of cellulose acetate with polyacrylic acid reinforced with carbon nanotubes and its applicability for chromium removal. *Int J Polym Sci*, 201 (2015).
38. Y. Cai, J. Lv and J. Feng, Spectral Characterization of Four Kinds of Biodegradable Plastics: Poly (Lactic Acid), Poly (Butylenes Adipate-Co-Terephthalate), Poly (Hydroxybutyrate-Co-Hydroxyvalerate) and Poly (Butylenes Succinate) with FTIR and Raman Spectroscopy. *J Polym Environ* **21**(1), 108-114 (2013).
39. K. Zhang, A. Feldner, S. Fischer, FT Raman spectroscopic investigation of cellulose acetate. *Cellulose* **18**(4), 995-1003 (2011).
40. J.R. Scherer, G.F. Bailey, S. Kint, R. Young, D.P. Malladi and B. Bolton, Water in polymer membranes. 4. Raman scattering from cellulose acetate films. *J Phys Chem* **89**(2), 312-319 (1985).
41. M. Yan, S. Li, M. Zhang, C. Li, F. Dong and W. Li, Characterization of surface acetylated nanocrystalline cellulose by single-step method. *BioResources* **8**(4), 6330-6341 (2013).
42. L.P. Terrazas-Bandala, L.A. Manjarrez-Nevárez, A. Duarte-Möller, M.D.L. Ballinas-Casarrubias, G. González-Sánchez, SEM analysis of composite cellulose acetate membranes for separation operations. *Microsc Microanal* **11**(S02), 774-775 (2005).
43. M. Jonoobi, J. Harun, A.P. Mathew and K. Oksman, Mechanical properties of cellulose nanofiber (CNF) reinforced polylactic acid (PLA) prepared by twin screw extrusion. *Compos Sci Technol* **70**(12), 1742-1747 (2010).

